

TNF- α Mediates Diabetes-Enhanced Chondrocyte Apoptosis During Fracture Healing and Stimulates Chondrocyte Apoptosis Through FOXO1

Rayyan A Kayal,^{1*} Michelle Siqueira,^{1*} Jazia Alblowi,^{1*} Jody McLean,² Nanarao Krothapalli,¹ Dan Faibish,¹ Thomas A Einhorn,² Louis C Gerstenfeld,² and Dana T Graves³

¹Department of Periodontology and Oral Biology, Boston University School of Dental Medicine, Boston, MA, USA

²Department of Orthopedic Surgery, Boston University School of Medicine, Boston, MA, USA

³Department of Periodontics, University of Medicine and Dentistry of New Jersey, Newark, NJ, USA

ABSTRACT

To gain insight into the effect of diabetes on fracture healing, experiments were carried out focusing on chondrocyte apoptosis during the transition from cartilage to bone. Type 1 diabetes was induced in mice by multiple low-dose streptozotocin injections, and simple transverse fractures of the tibia or femur was carried out. Large-scale transcriptional profiling and gene set enrichment analysis were performed to examine apoptotic pathways on total RNA isolated from fracture calluses on days 12, 16, and 22, a period of endochondral bone formation when cartilage is resorbed and chondrocyte numbers decrease. Tumor necrosis factor α (TNF- α) protein levels were assessed by ELISA and caspase-3 by bioactivity assay. The role of TNF was examined by treating mice with the TNF-specific inhibitor pegsunercept. In vitro studies investigated the proapoptotic transcription factor FOXO1 in regulating TNF-induced apoptosis of chondrogenic ATDC5 and C3H10T1/2 cells as representative of differentiated chondrocytes, which are important during endochondral ossification. mRNA profiling revealed an upregulation of gene sets related to apoptosis in the diabetic group on day 16 when cartilage resorption is active but not day 12 or day 22. This coincided with elevated TNF- α protein levels, chondrocyte apoptosis, enhanced caspase-3 activity, and increased FOXO1 nuclear translocation ($p < .05$). Inhibition of TNF significantly reduced these parameters in the diabetic mice but not in normoglycemic control mice ($p < .05$). Silencing FOXO1 using siRNA in vitro significantly reduced TNF-induced apoptosis and caspase activity in differentiated chondrocytes. The mRNA levels of the proapoptotic genes *caspase-3*, *caspase-8*, *caspase-9*, and *TRAIL* were significantly reduced with silencing of FOXO1 in chondrocytic cells. Inhibiting *caspase-8* and *caspase-9* significantly reduced TNF-induced apoptosis in chondrogenic cells. These results suggest that diabetes causes an upregulation of proapoptotic genes during the transition from cartilage to bone in fracture healing. Diabetes increased chondrocyte apoptosis through a mechanism that involved enhanced production of TNF- α , which stimulates chondrocyte apoptosis and upregulates mRNA levels of apoptotic genes through FOXO1 activation. © 2010 American Society for Bone and Mineral Research.

KEY WORDS: APOPTOSIS; BONE; CELL DEATH; CHONDROCYTE; CARTILAGE; CYTOKINE; FRACTURE; FORKHEAD; NUCLEAR LOCALIZATION; TRANSCRIPTION FACTOR

Introduction

Diabetes has as one of its complications osteopenia associated with decreased bone mineral density (BMD).^(1–6) Several mechanisms have been suggested for osteopenia caused by type 1 diabetes, including reduced bone formation supported by decreased levels of serum osteocalcin.⁽⁶⁾ It also may be due to increased bone resorption, indicated by enhanced serum levels of type 1 collagen cross-linked carboxy-terminal telopeptide.⁽¹⁾

Alternatively, reduced numbers of osteoblasts and decreased production of extracellular matrix proteins associated with decreased production of growth factors such as insulin-like growth factor 1 (IGF-1) may account for diminished bone formation.^(1,2) Animal models are consistent with human studies demonstrating increased basal levels of bone resorption associated with increased expression of TRACP and cathepsin K, as well as decreased markers of bone formation such as alkaline phosphatase.^(7,8)

Received in original form March 20, 2009; revised form January 5, 2010; accepted February 2, 2010. Published online February 8, 2010.

Address correspondence to: Dana T Graves, DDS, DMSc, Department of Periodontics, University of Medicine and Dentistry, 110 Bergen Street, C781, Newark, NJ 07101, USA. E-mail: gravesdt@umdnj.edu

*The first three authors contributed equally to this article.

Additional Supporting Information may be found in the online version of this article.

Journal of Bone and Mineral Research, Vol. 25, No. 7, July 2010, pp 1604–1615

DOI: 10.1002/jbmr.59

© 2010 American Society for Bone and Mineral Research

Diabetes has been shown to significantly impair fracture healing. Case reports and clinical investigations have reported delayed union or increased healing time in diabetic subjects compared with matched controls.^(9,10) It has been reported that diabetic animals had a significantly smaller amount of new bone on days 14 and 21 after fracture than normal and insulin-treated animals, which was associated with decreased Ca deposition.⁽¹¹⁾ The DNA content of diabetic fracture calluses is decreased by 40% compared with normal controls.⁽⁹⁾ This is an indication that the diabetic calluses have decreased cellularity compared with normal calluses. In addition, the same study reported reduced bone matrix formation, represented by a 50% to 55% decrease in the collagen content of the calluses of diabetic animals. Diabetic animals have significantly smaller calluses with smaller bone and cartilage areas than normoglycemic animals.⁽¹²⁾ In addition to having an impact on bone formation, diabetes affects the transition from cartilage to bone during fracture repair by accelerating the loss of cartilage, which serves as an anlage for endochondral bone formation.^(13,14) The greater loss of cartilage in diabetic fracture calluses is associated with increased mRNA levels of proresorptive factors and diabetes-enhanced osteoclastogenesis.⁽¹³⁾

Chondrocyte apoptosis is an important event in the transition from cartilage to bone during fracture healing and growth of long bones.⁽¹⁵⁾ This process is induced by cytokines such as tumor necrosis factor α (TNF- α) and interleukin 1 β (IL-1 β).^(16,42) Chondrocytes have been shown to produce RANKL and may regulate osteoclastogenesis at growth plates to remove calcified matrix in response to bone morphogenetic protein 2 (BMP-2).⁽¹⁷⁾ Apoptosis of chondrocytes may be important for matrix degradation.⁽¹⁶⁾ Apoptosis and the associated activation of the caspase proteolytic cascade has been detected in parallel with matrix metalloproteinase (MMP) expression and may be one mechanism for the activation of MMPs.⁽¹⁷⁾ Moreover, apoptosis of hypertrophic chondrocytes is associated with secretion of osteogenic growth factors such as transforming growth factor β (TGF- β) and angiogenic factors such as fibroblast growth factor 2 (FGF-2) and may be important in regulating the early steps in bone formation as cartilage matrix is resorbed.⁽¹⁸⁾ Similarly, apoptotic vesicles produced by chondrocytes are rich in alkaline phosphatase and may regulate the calcification of osteoid matrix.⁽¹⁷⁾

Diabetes enhances the expression of proinflammatory factors in a number of conditions. In some cases, this is tied to increased NF- κ B activity, which is directly antiapoptotic. In contrast, the transcription factor FOXO1 is proapoptotic and stimulated under conditions present in diabetes, such as increased levels of inflammatory mediators, advanced glycation end products, and reactive oxygen species and decreased Akt activity.^(19–21) Our laboratory has shown that diabetes increases FOXO1 DNA binding activity during fracture healing and that diabetes enhances FOXO1 nuclear translocation in chondrocytes *in vivo*.⁽²²⁾ In numerous cell types, activation of the FOXO family leads to apoptosis, particularly when its expression or activation is prolonged.^(23,24) Some of the FOXO-responsive genes are apoptotic effectors such as TNF- α and FAS ligand.^(19,25)

To gain insight into the effect of diabetes on fracture healing, large-scale transcriptional profiling analysis and gene set enrichment analysis were performed on total mRNA isolated from

fracture calluses at various stages during fracture healing in control and diabetic mice. The effect of diabetes on the expression of various functional ontologies of gene expression then was assessed by gene set enrichment analysis (GSEA) focusing on apoptotic pathways. In order to validate changes in apoptotic mechanisms in chondrocyte, tissues were examined by histologic assessment. The potential regulatory role that TNF- α carries in mediating accelerated chondrocyte apoptosis was investigated by treating mice with the TNF-specific inhibitor pegsunercept. Finally, since TNF-induced apoptosis is mediated through FOXO1 in fibroblasts and osteoblasts and diabetes increases FOXO1 activity,^(19,22,26) we examined the relationship between FOXO1 and chondrocyte apoptosis *in vitro* using siRNA.

Materials and Methods

Induction of type 1 diabetes

All experiments were approved by the Boston University Medical Center Institutional Animal Care and Use Committee (IACUC). Eight-week-old male CD-1 mice purchased from Charles River Laboratories (Wilmington, MA, USA) were rendered diabetic by an intraperitoneal (i.p.) injection of streptozotocin (40 mg/kg; Sigma, St. Louis, MO, USA) in 10 mM of citrate buffer daily for 5 days.⁽²⁷⁾ Control mice were treated identically with vehicle alone, 10 mM of citrate buffer. A group of diabetic mice was treated with the TNF- α inhibitor pegsunercept by i.p. injection (4 mg/kg) every 3 days starting on day 10 after fracture until the time of euthanasia. Animals were considered to be diabetic when serum glucose levels exceeded 250 mg/dL (Accu-Chek, Roche Diagnostics, Indianapolis, IN, USA). Glycosylated hemoglobin levels were measured at the time of euthanasia by Glyco-tek Affinity Chromatography (Helena Laboratories, Beaumont, TX, USA). The diabetic group had values that were typically approximately 12%, and normoglycemic mice had values that were approximately 6%. Average blood glucose levels of diabetic animals were approximately three times higher than the values found in normoglycemic mice.

Tibial and femoral fractures

All studies were performed on male mice that were diabetic for at least 3 weeks prior to fracture. A simple transverse closed fracture of the tibia or femur was performed in separate animals, as described previously.^(13,28,29) For tibial fractures, an incision was made on the medial aspect of the knee, and the articular surface of the tibia was exposed. In the femoral fractures, the incision was made lateral to the knee, and the tendon for the quadriceps femoris muscle was pushed medially, exposing the articular surface of the femur. Access to the medullary canal was gained with a 25-gauge needle, and a 27-gauge spinal needle was inserted for fixation. After closure of the incision, a fracture was created by blunt trauma. Fractures were examined radiographically, and any fractures not consistent with standardized placement criteria (mid-diaphyseal) or grossly comminuted were excluded. Animals were subsequently euthanized at 12, 16, and 22 days after fracture for the tibias and after 10, 16, and 22 days after fracture for the femurs.

Histology and histomorphometric analysis

The femurs with a small amount of surrounding muscle and soft tissues were fixed for 72 hours in cold 4% paraformaldehyde and decalcified for 2 weeks by incubation in cold Immunocal (Decal Corporation, Congers, NY, USA). After decalcification, specimens were embedded in paraffin, sectioned at 5 μm , and prepared for staining. Apoptotic cells were detected by the TUNEL assay (ApopTag Peroxidase In Situ Apoptosis Detection Kit, Chemicon International, Temecula, CA, USA) on sections stained with safranin-O/fast green to distinguish cartilage. For each data point, there were six to eight specimens. One examiner under blinded conditions made the measurements, with the results confirmed by a second examiner.

FOXO1 nuclear localization

Sections were prepared as described earlier and incubated overnight with anti-FOXO1 antibody (Santa Cruz Biotech, Santa Cruz, CA, USA) or matched negative control antibody. Primary antibody to FOXO1 was detected by a Cy5-tagged secondary antibody. Propidium iodide nuclear stain was included in the mounting medium. FOXO1 nuclear localization was detected by confocal laser scanning microscopy at a focal plane that bisected the nuclei (Axiovert-100M, Carl Zeiss, Thornwood, NY, USA). Cy5, propidium iodide, and phase-contrast images (original magnification $\times 400$) of the same field were captured digitally. The cartilage area in nonoverlapping fields was analyzed, and the percent chondrocytes with unambiguous nuclear localization was assessed by comparing FOXO1/Cy5, propidium iodide, and merged and phase-contrast images. For each group, $n = 5$ to 6 specimens. Results were confirmed by a second examiner.

mRNA profiling of gene sets that regulate apoptosis

After euthanasia, fractured tibial calluses were carefully dissected, removing all muscle and noncallus tissue, and immediately frozen in liquid nitrogen. Total RNA was extracted with Trizol (Life Technologies, Rockville, MD, USA) from pulverized frozen tissue and further purified by an RNAeasy MinElute Cleanup Kit (Qiagen, Valencia, CA, USA). The concentration and integrity of the extracted RNA were verified by 260/280-nm spectrophotometry and denaturing agarose gel electrophoresis with ethidium bromide staining.

mRNA profiling was carried out using a PGA Mouse Version 1.1 array (MGH-ParaBiosys, Boston, MA). Microarray probe preparation, hybridization, and reading of fluorescent intensity were performed by the Massachusetts General Hospital Microarray Core Facility (Cambridge, MA, USA). All slides were coprinted with an internal "alien" sequence that has no sequence homologues in the mouse genome. Slide printing, array labeling, hybridization, and slide reading were performed at the Massachusetts General Hospital Genomics Core Facility, as described previously.⁽³⁰⁾ All slides were quality control tested and contained appropriate positive and negative control sequences for data analysis. The alien gene in these studies serves as both a genome-extrinsic sequence and a universal in-spot reference. In the experiments reported here, all microarrays were printed in such a way that an alien 70mer probe was coprinted with each

gene specific probe such that the alien was at a final concentration of 10% of the murine gene oligonucleotide. The data were normalized by scaling all individual intensities such that mean total intensities were the same for all comparative samples (normal, diabetic, and alien) within a single array and across replicates. Using the intensity reading, background was calculated locally per spot and subtracted from the intensity measurement of each hybridized spot. The ratio of normal to alien was calculated first. Using this ratio, all outliers for a given gene were discarded. The standard \log_{10} of diabetic versus normal and diabetic versus alien for each spot was calculated, and the distribution of the log ratios was obtained from combined replicates per time point. The data are combined using the geometric mean of four replicate ratios.

Microarray data were analyzed using GSEA software and the Molecular Signature Database (MSigDB) as described in ref.⁽³¹⁾, which can be accessed at the following Web site: www.broad.mit.edu/gsea/. Genes were first ranked based on the correlation between their expression and the class distinction. An enrichment score then was calculated that reflects the degree to which a gene is overrepresented at the extremes (top or bottom) of the entire ranked list. Statistical significance (p value) and false discovery rate (FDR) of that enrichment score then were calculated. This statistical analysis determines whether a gene set is significantly upregulated or downregulated in the experimental sample compared with a control. Gene sets with an FDR of less than 25% and a nominal p value of less than .05 were considered significant.⁽³¹⁾ Genes that contributed to a significant difference in pathways related to apoptosis were identified by the GSEA software and further screened for significance by Student's t test ($p < .05$), as well as for a threshold change of 1.5 increase or decrease in the diabetic versus normoglycemic microarray values, as described in ref.⁽³²⁾.

For *TNF- α* , *TRAIL*, and *caspase-4* mRNA levels obtained with microarrays were validated by real-time PCR using primers and probe sets purchased from Applied Biosystems (Foster City, CA, USA), as described previously.⁽¹⁹⁾ Experiments were carried out on three sets of samples, and each set represented three animals for $n = 9$. For a given experiment, RNA was combined and TaqMan reagents were used for first-strand cDNA synthesis and amplification. Results were normalized with an 18S ribosomal primer and probe set. Each experiment was performed three times, and the results from the three separate experiments were combined to derive mean values. For a given gene, the expression for each group was set relative to the value obtained for the normoglycemic control animals on day 12.

TNF- α and caspase-3 protein levels

Frozen tissue was pulverized and incubated with cold lysis buffers containing protease inhibitors (Pierce, Rockford, IL, USA) and tested for TNF- α (R&D, Minneapolis, MN, USA) and caspase-3 activity with a luminescent kit (Promega, San Luis Obispo, CA, USA). Each assay was carried out three times with similar results.

In vitro experiments

In vitro experiments were carried out with cell lines that had a chondrogenic phenotype induced by BMP stimulation. Experiments were performed with ATDC5 (murine chondrogenic cell

line) and C3H10T1/2 (murine mesenchymal stem cell line) cells obtained from the American Type Culture Collection (Rockville, MD, USA). Pluripotent C3H10T1/2 cells have been shown to undergo chondrogenic differentiation in the presence of BMP-2.^(33,34) ATDC5 cells undergo multistep chondrogenic differentiation, in which they differentiate into type II and X collagen-expressing cells.^(35,36) Thus, with BMP-2 stimulation, both C3H10T1/2 and ATDC5 cells exhibit a hypertrophic chondrocyte phenotype.⁽³⁷⁾ Cells were grown in a 1:1 mixture of DMEM and Ham's F-12 medium (Cellgro, Manassas, VA, USA) at 37°C in a humidified atmosphere of 5% CO₂ in air. The medium was supplemented with 5% fetal bovine serum (FBS) for ATDC5 and 10% FBS for C3H10T1/2 and 1% penicillin/streptomycin. To induce differentiation into chondrocytes, ATDC5 cells were incubated in 0.5% FBS medium with 200 ng/mL BMP-2 (Peprotech, Rocky Hill, NJ, USA) for 6 days, whereas C3H10T1/2 cells were incubated in 0.5% FBS and 100 ng/mL BMP-2 for 4 days. The chondrogenic phenotype was verified by BMP-2-induced *collagen II* and *collagen X* mRNA levels measured by real-time PCR.

To inhibit reactive oxygen species (ROS), cells were plated in six-well plates and were preincubated with 5 or 10 mM of *N*-acetyl-L-cysteine (NAC) (Sigma-Aldrich) for 2 hours or with 5 or 10 mM of Trolox (vitamin E analogue; Calbiochem, Gibbstown, NJ, USA) for 30 minutes, followed by TNF- α stimulation (20 ng/mL) as described earlier. To inhibit caspases, cells were plated in six-well plates and were incubated with either 50 μ M of caspase-8 inhibitor IETD-FMK (RandD Systems, Minneapolis, MN, USA),

50 μ M of caspase-9 inhibitor LEHD-FMK (RandD Systems), or a mixture of both for 24 hours combined with 20 ng/mL of TNF- α .

ATDC5 and C3H10T1/2 cells were transferred to six-well plates and, when 70% confluent, were transfected with 148.5 ng/mL of FOXO1 siRNA or scrambled siRNA with HiPerFect (Qiagen, Valencia, CA, USA) in medium supplemented with 0.25% FBS for 24 hours. The target sequence of FOXO1 siRNA was CCA GCT ATA AAT GGA CAT TTA. After another 24 hours in low-serum medium, cells were stimulated with 20 ng/mL of TNF (Peprotech) for 6 hours. Total RNA was extracted using QIA shredder Mini Spin Columns and RNeasy Mini Kit (Qiagen). MultiScribe Reverse Transcriptase (Applied Biosystems) was used to convert RNA to cDNA, and real-time PCR was performed using Taqman primers and probe sets (Applied Biosystems). Nuclear and cytoplasmic proteins were extracted from cell lysate using NE-PER Nuclear and Cytoplasmic Extraction Reagents Kit (Pierce), and a protease inhibitor cocktail was added (Pierce). Bicinchoninic acid protein assay (BCA) was used to measure protein content of the nuclear and cytoplasmic extract (Pierce). FOXO1 DNA-binding activity was measured using a transcription factor ELISA kit for FOXO1 (Active Motif, Carlsbad, CA) following the manufacturer's instructions. Apoptosis was measured by the use of a Cell Death Detection ELISA kit (Roche), which detects the amount of histone-associated DNA fragments in mono- and oligonucleosomes, which are known markers of apoptotic cells. Caspase-3/7 activity was measured by a luminometric substrate (Promega) following manufacturer's instructions.

Table 1. Gene Set Enrichment Analysis for Pathways Involved in Apoptosis

Normal vs diabetic		Day 12				Day 16				Day 22			
		Upregulated in normal		Upregulated in diabetic		Upregulated in normal		Upregulated in diabetic		Upregulated in normal		Upregulated in diabetic	
Apoptotic gene sets	No. of genes	<i>p</i> Value	FDR	<i>p</i> Value	FDR	<i>p</i> Value	FDR	<i>p</i> Value	FDR	<i>p</i> Value	FDR	<i>p</i> Value	FDR
Passerini apoptosis	34	N/S	N/S	N/S	N/S	N/S	N/S	0*	.07*	N/S	N/S	N/S	N/S
Apoptosis Kegg	37	N/S	N/S	N/S	N/S	N/S	N/S	0*	.11*	N/S	N/S	N/S	N/S
Apoptosis	57	N/S	N/S	N/S	N/S	N/S	N/S	0*	.13*	N/S	N/S	N/S	N/S
Death pathway	28	N/S	N/S	N/S	N/S	N/S	N/S	.01*	.19*	N/S	N/S	N/S	N/S
Cell death	13	N/S	N/S	N/S	N/S	N/S	N/S	N/S	N/S	N/S	N/S	N/S	N/S
SA programmed cell death	11	N/S	N/S	N/S	N/S	N/S	N/S	N/S	N/S	N/S	N/S	N/S	N/S
Vanasse BCL2 targets	77	0*	.01*	N/S	N/S	N/S	N/S	0*	.02*	0*	.21*	N/S	N/S
NF- κ B pathway	21	N/S	N/S	N/S	N/S	N/S	N/S	0*	.09*	N/S	N/S	N/S	N/S
TNF and FAS network	19	N/S	N/S	N/S	N/S	N/S	N/S	0*	.10*	N/S	N/S	N/S	N/S
TNFA NF- κ B dep up	16	N/S	N/S	N/S	N/S	N/S	N/S	0*	.07*	N/S	N/S	N/S	N/S
FAS pathway	23	N/S	N/S	N/S	N/S	N/S	N/S	N/S	N/S	N/S	N/S	N/S	N/S
ST FAS signaling pathway	56	N/S	N/S	N/S	N/S	N/S	N/S	.01*	.17*	N/S	N/S	N/S	N/S
Caspase pathway	20	N/S	N/S	N/S	N/S	N/S	N/S	0*	.10*	N/S	N/S	N/S	N/S
SA caspase cascade	15	N/S	N/S	N/S	N/S	N/S	N/S	N/S	N/S	N/S	N/S	N/S	N/S
PKC pathway	6	N/S	N/S	N/S	N/S	N/S	N/S	.01*	.14*	N/S	N/S	N/S	N/S
Passerini oxidation	16	N/S	N/S	N/S	N/S	N/S	N/S	0*	.11*	N/S	N/S	N/S	N/S
JNK up	25	N/S	N/S	N/S	N/S	N/S	N/S	0*	.07*	N/S	N/S	N/S	N/S
Ceramide pathway	20	N/S	N/S	N/S	N/S	N/S	N/S	N/S	N/S	N/S	N/S	N/S	N/S
BAD pathway	18	N/S	N/S	N/S	N/S	N/S	N/S	N/S	N/S	N/S	N/S	N/S	N/S
P53 pathway	15	N/S	N/S	N/S	N/S	N/S	N/S	N/S	N/S	N/S	N/S	N/S	N/S
P53 hypoxia pathway	15	N/S	N/S	N/S	N/S	N/S	N/S	N/S	N/S	N/S	N/S	N/S	N/S

Table 2. mRNA Levels Obtained by Microarray or Real-Time PCR

	Real-time PCR (relative intensity)			Microarray (relative intensity)		
	Normal	Diabetic	Fold change	Normal	Diabetic	Fold change
<i>TNF-α</i>	2.5 \pm 0.1	9.5 \pm 1.1	3.8	2.3 \pm 0.3	4.6 \pm 0.6	2.0
<i>TRAIL</i>	1.2 \pm 0.1	3.0 \pm 0.6	2.5	3.8 \pm 0.8	6.5 \pm 1.4	1.7
<i>Caspase-4</i>	1.1 \pm 0.1	2.0 \pm 0.1	1.8	1.8 \pm 0.1	3.4 \pm 0.4	1.9

Note: Microarray analysis or real-time PCR was carried out three times, as described earlier, on day 16 fracture-healing specimens. The fold change represents the values of the diabetic compared with normoglycemic specimens. Each value represents the mean \pm SEM of triplicate samples. In each case, the diabetic value was significantly higher than the normoglycemic value ($p < .05$).

Statistical analysis

Data represent mean values \pm SEM. Statistical significance between diabetic and normoglycemic groups for a given parameter was established by Student's *t* test at the $p < .05$ level. ANOVA with Scheffe's post hoc test was used to analyze differences between multiple groups at the same time point.

Results

To assess the impact of diabetes on apoptosis in healing fractures, large-scale transcriptional profiling analysis and GSEA were performed on RNA isolated from fracture calluses at various stages during fracture healing in control and diabetic

mice. A striking result was that on day 16 after fracture, diabetes enhanced 13 of 21 gene sets associated with apoptosis (Table 1). These gene sets were frequently associated with the extrinsic pathway, such as TNF and Fas. Gene sets associated with the intrinsic pathway tended to not be upregulated by diabetes, including the ceramide, p53, and BAD pathways. In contrast, on days 12 and 22 after fracture, diabetes had relatively little effect on upregulation of the apoptotic gene sets, suggesting that the major effects of altered apoptotic regulation occurred in the later hypertrophic period of chondrocyte differentiation, during endochondral bone formation that is seen in the callus tissues. Individual proapoptotic genes that significantly contributed to the entire set being upregulated in the diabetic group were

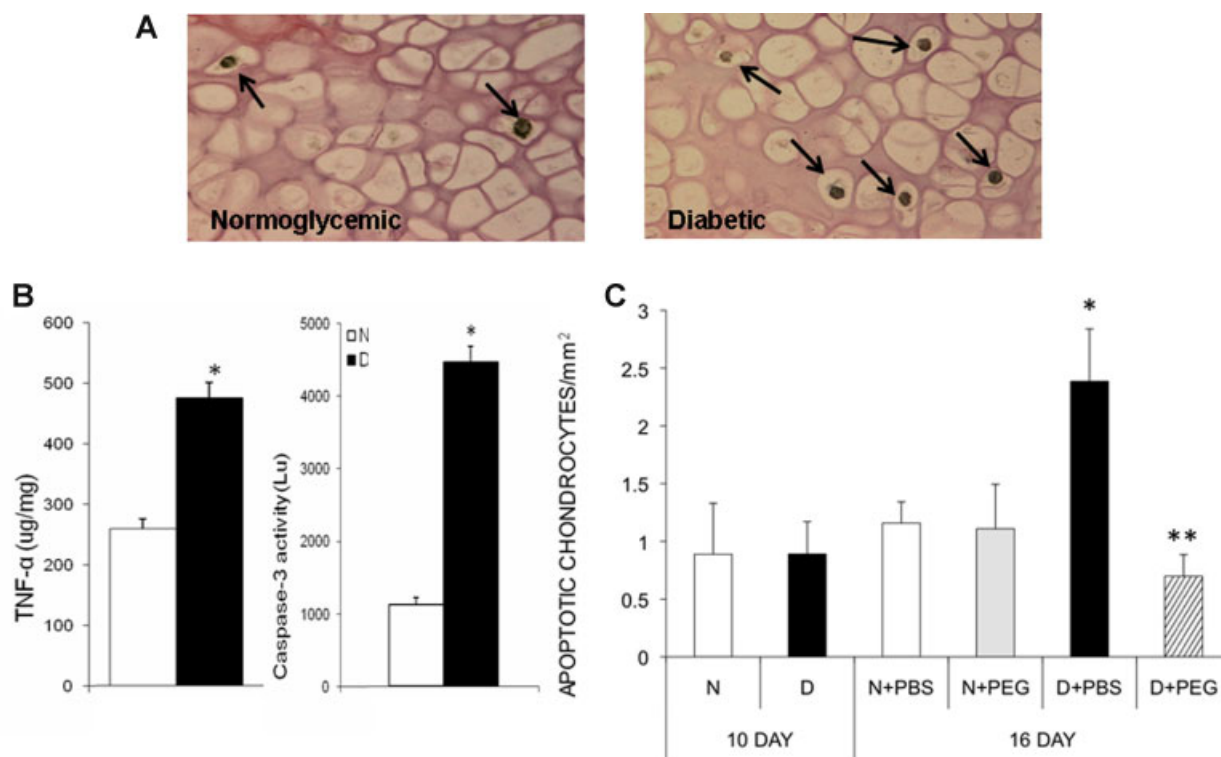


Fig. 1. TNF- α protein levels and caspase-3 activity are increased by diabetes in healing fractures, and TNF inhibition reverses diabetes-enhanced chondrocyte apoptosis. (A) Histologic images of cartilage from normoglycemic and diabetic mice (original magnification $\times 400$). Arrows indicate TUNEL⁺ chondrocytes. (B) Protein was extracted from fracture calluses and tested for TNF- α by ELISA (right panel) and for caspase-3 activity by a luminescent assay (left panel). Each value represents the mean \pm SEM of triplicate samples, and each assay was carried out three times with similar results. *A significant difference between normoglycemic and diabetic groups ($p < .05$). Sections from fracture calluses were examined by the TUNEL assay and counterstained with safranin-O/fast green to identify cartilage. (C) Quantitative analysis of TUNEL⁺ cells in diabetic mice (D), matched normoglycemic control mice (N). Normoglycemic or diabetic mice were treated with pegsunercept (PEG) or vehicle alone (PBS). Data are expressed as mean \pm SEM. *A significant difference from the diabetic group ($p < .05$). **Significant difference between diabetic and pegsunercept-treated diabetic mice ($p < .05$).

identified by leading-edge analysis. Proapoptotic genes that appeared in more than three gene sets included *NFκB1α*, *TRAF-1*, *TRAF-2*, *TRAF-3*, *TNF-α*, *MCL-1*, *TNF receptor 1α*, *APAF-1*, and *caspase-1*.

Candidate mRNA levels of selected apoptotic genes (*TNF-α*, *TRAIL*, and *caspase-4*) were validated by real-time qRT-PCR (Table 2). The 16-day time point was chosen for this comparison because it is the time point where most changes were observed. Microarray assessment of *TNF-α*, *TRAIL*, and *caspase-4* expression had shown that the mRNA levels of these genes were enhanced in diabetic animals by 1.7- to 2.0-fold ($p < .05$). When examined by real-time PCR the results indicated a 1.8- to 3.8-fold elevation in the diabetic group, thus confirming increased mRNA levels ($p < .05$).

Comparison studies of callus and cartilage area demonstrated that diabetes resulted in a decrease in callus and cartilage area, and *TNF-α* inhibition resulted in reversal of the effect of diabetes ($p < .05$; Supplemental Table S1). Subsequent studies were carried out to functionally assess chondrocyte apoptosis, *TNF-α* at the protein level, and *caspase-3* at the level of activity on day 16. Increased TUNEL⁺ chondrocytes, which were predominantly hypertrophic chondrocytes, were consistently observed at higher

levels in the diabetic group (Fig. 1A). Higher levels of apoptosis coincided with a 1.8-fold higher level of *TNF-α* and a 3.9-fold higher level of *caspase-3* activity in the fracture calluses in the diabetic group compared with the normoglycemic group ($p < .05$; Fig. 1B). The increase in chondrocyte apoptosis was established by quantitative analysis. Diabetes enhanced chondrocyte apoptosis on day 16 ($p < .05$) but did not on day 10 (Fig. 1C). Given that diabetic mice had elevated *TNF-α* protein and mRNA levels and that gene sets related to *TNF* signaling were enhanced by diabetes (Table 1), a potential mechanism for the increased levels of apoptosis that were seen in diabetes was investigated by treating mice with the *TNF*-specific inhibitor pegsunercept. When diabetic mice were treated with pegsunercept, there was a 76% decrease in chondrocyte apoptosis in the diabetic group so that the levels returned to those seen in normal animals ($p < .05$; Fig. 1C). In contrast, there was no significant difference in chondrocyte apoptosis in normoglycemic mice treated with pegsunercept compared with vehicle-treated controls ($p > .05$). On day 22, the amount of cartilage was minimal, precluding the accurate counting of apoptotic chondrocytes.

To determine whether *FOXO1* was affected by diabetes, we examined *FOXO1* nuclear localization that occurred in

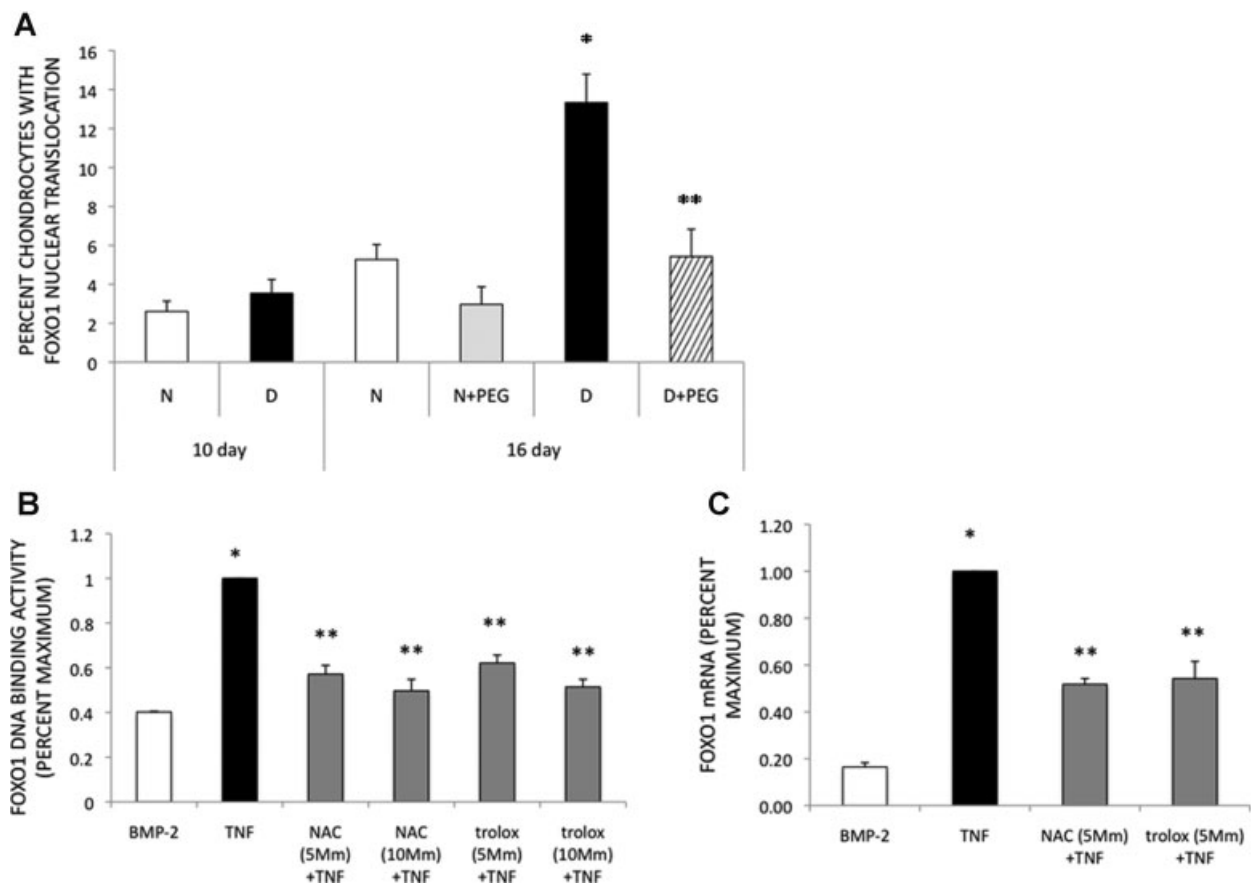


Fig. 2. Diabetes increases *FOXO1* nuclear localization in chondrocytes of healing fractures, and inhibition of ROS reduces *TNF-α*-stimulated *FOXO1* DNA binding and *FOXO1* mRNA. (A) Transverse sections from calluses were incubated with anti-*FOXO1* IgG or matched-control IgG, and nuclear localization was assessed by confocal scanning laser microscopy by counting the percentage of chondrocytes with unambiguous *FOXO1* nuclear localization. ATDC5 cells were stimulated with BMP-2 and *TNF-α*. This was followed by treatment of cells by the ROS inhibitors NAC and Trolox. (B) *FOXO1* DNA-binding activity was measured using ELISA. (C) *FOXO1* mRNA was isolated and measured using qPCR. Data are expressed as mean \pm SEM. *A significant difference from the diabetic group and a significant increase with *TNF-α* stimulation ($p < .05$). **Significant difference between diabetic and pegsunercept-treated diabetic mice and significant reduction with ROS inhibitors ($p < .05$).

chondrocytes in diabetic fractures by confocal laser scanning microscopy (Supplemental Fig. S1). When FOXO1 is activated, it translocates to the nucleus, and on deactivation, it is quickly transported out of the nucleus. There were no differences in FOXO1 nuclear localization between diabetic mice and normoglycemic mice on day 10 ($p > .05$). On day 16, diabetes caused a 2.5-fold increase in the percentage of chondrocytes with FOXO1 nuclear localization compared with matched normoglycemic controls ($p < .05$; Fig. 2A). Inhibition of TNF in the diabetic group resulted in a 59.3% decrease in the percentage of chondrocytes that had FOXO1 nuclear localization ($p < .05$). In contrast, TNF inhibition had no significant effect on FOXO1 nuclear localization in normoglycemic mice ($p > .05$).

To better understand the mechanistic process of chondrocyte apoptosis, TNF- α -stimulated chondrocyte apoptosis was investigated in vitro by examining the role of FOXO1, which has been shown to mediate proapoptotic gene expression.^(20,21) RNAi studies were performed in BMP-stimulated ATDC5 cells that have a chondrogenic phenotype.⁽³⁶⁾ TNF- α increased FOXO1 mRNA levels 3.8-fold and DNA-binding activity almost 2-fold ($p < .05$; Table 3). When transfected with siRNA and then stimulated with TNF- α , FOXO1 mRNA levels were reduced by 73% compared with scrambled siRNA ($p < .05$). TNF- α -stimulated FOXO1 DNA-binding activity was reduced 63% by FOXO1 siRNA compared with scrambled siRNA ($p < .05$). Scrambled siRNA had no effect on FOXO1 mRNA or DNA-binding activity compared with cells that were not transfected (Table 3).

Since FOXO1 has been linked to oxidative stress,⁽¹⁷⁾ we determined whether inhibition of reactive oxygen species (ROS) affected the capacity of TNF- α to induce FOXO1. When ROS was inhibited by NAC or by Trolox, the level of FOXO1 DNA-binding activity was reduced by 60%, which represents a 90% decrease in the amount stimulated by TNF- α (Fig. 2A, and 2B). FOXO1 mRNA levels were reduced by 50% by either of the ROS inhibitors, which represents an 80% decrease in the mRNA levels stimulated by TNF- α (Fig. 2C).

The role of FOXO1 on TNF- α -induced apoptosis and caspase activity was assessed by siRNA. TNF- α stimulated a 5-fold

Table 3. FOXO1 mRNA Levels and DNA-Binding Activity After Silencing With FOXO1 siRNA

	FOXO1 mRNA	FOXO1 DNA-binding activity
Negative control	1.00 \pm 0.00	1.00 \pm 0.0
BMP	0.93 \pm 0.08	1.0 \pm 0.1
BMP + TNF	3.7 \pm 0.3*	1.9 \pm 0.2*
BMP + TNF + SCR siRNA	3.4 \pm 0.1*	1.8 \pm 0.2*
BMP + TNF + FOXO1 siRNA	1.0 \pm 0.3**	0.7 \pm 0.1**

Note: ATDC5 cells were stimulated with BMP-2 and with TNF- α . This was followed by transfection with either FOXO1 siRNA or scrambled siRNA. mRNA then was isolated, and the level FOXO1 mRNA was measured. FOXO1 DNA-binding activity also was measured using ELISA. Data expressed as mean \pm SEM.

*Significant increase with TNF- α stimulation ($p < .05$).

**Significant reduction with FOXO1 siRNA ($p < .05$).

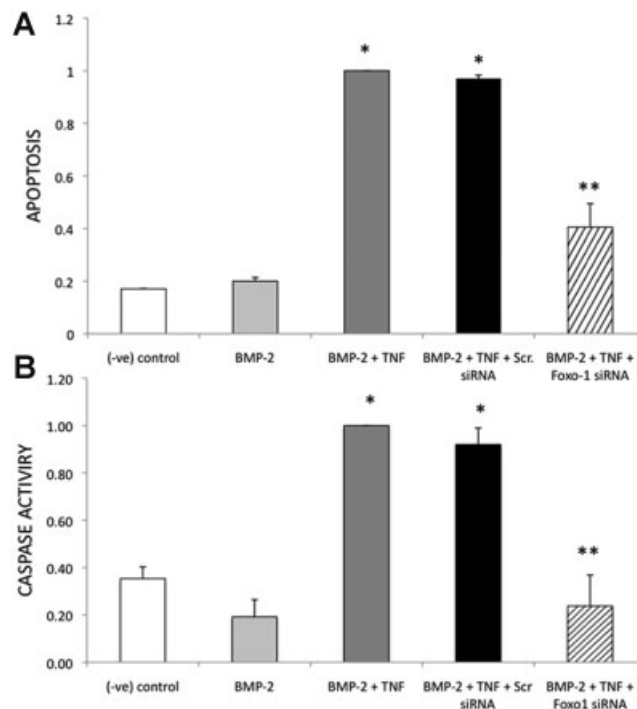


Fig. 3. TNF-induced apoptosis and caspase-3/7 activity in ATDC5 chondrogenic cells depends on FOXO1. BMP2-stimulated ATDC5 cells were transfected with either FOXO1 siRNA or scrambled siRNA and stimulated with TNF- α (20 ng/mL). (A) Apoptosis was measured by histone-associated cytoplasmic DNA and (B) caspase-3/7 activity with a luminescent substrate. The data presented are the mean of three independent experiments \pm SEM and are shown as percent of maximum stimulation. *Significant increase with TNF- α stimulation ($p < .05$). **Significant reduction with FOXO1 siRNA ($p < .05$).

increase in apoptosis, whereas FOXO1 knockdown decreased that level of apoptosis by almost 60% ($p < .05$; Fig. 3A). TNF- α also increased caspase-3/7 activity by 5-fold in ATDC5 cells compared with cells not incubated with TNF- α ($p < .05$). FOXO1 knockdown reduced caspase-3/7 activity by 75% when compared with cells transfected with scrambled siRNA ($p < .05$; Fig. 3B). There was no significant difference between scrambled siRNA transfected and nontransfected cells ($p > .05$).

To establish whether FOXO1 mediated TNF stimulation of proapoptotic genes, real-time PCR was carried out. TNF- α stimulated a 2-fold increase in caspase-3 mRNA in ATDC5, and FOXO1 knockdown decreased caspase-3 mRNA levels by over 60% compared with scrambled siRNA ($p < .05$; Fig. 4A). Caspase-8 mRNA was increased 1.9-fold in ATDC5 cells with TNF- α stimulation, which was reduced by 49% when FOXO1 was knocked down compared with scrambled siRNA ($p < .05$; Fig. 4B). Similar results were obtained with caspase-9, which was increased 2.3-fold in cells with TNF- α stimulation ($p < .05$). FOXO1 knockdown reduced this by 62% ($p < .05$; Fig. 4C). TRAIL was upregulated 200-fold in TNF- α -stimulated ATDC5 cells compared with cells without TNF- α ($p < .05$). FOXO1 siRNA reduced this by 59% compared with scrambled siRNA ($p < .05$; Fig. 4D). These results suggest that FOXO1 mediates mRNA levels of proapoptotic genes induced by TNF- α in cells with a hypertrophic chondrocyte phenotype.

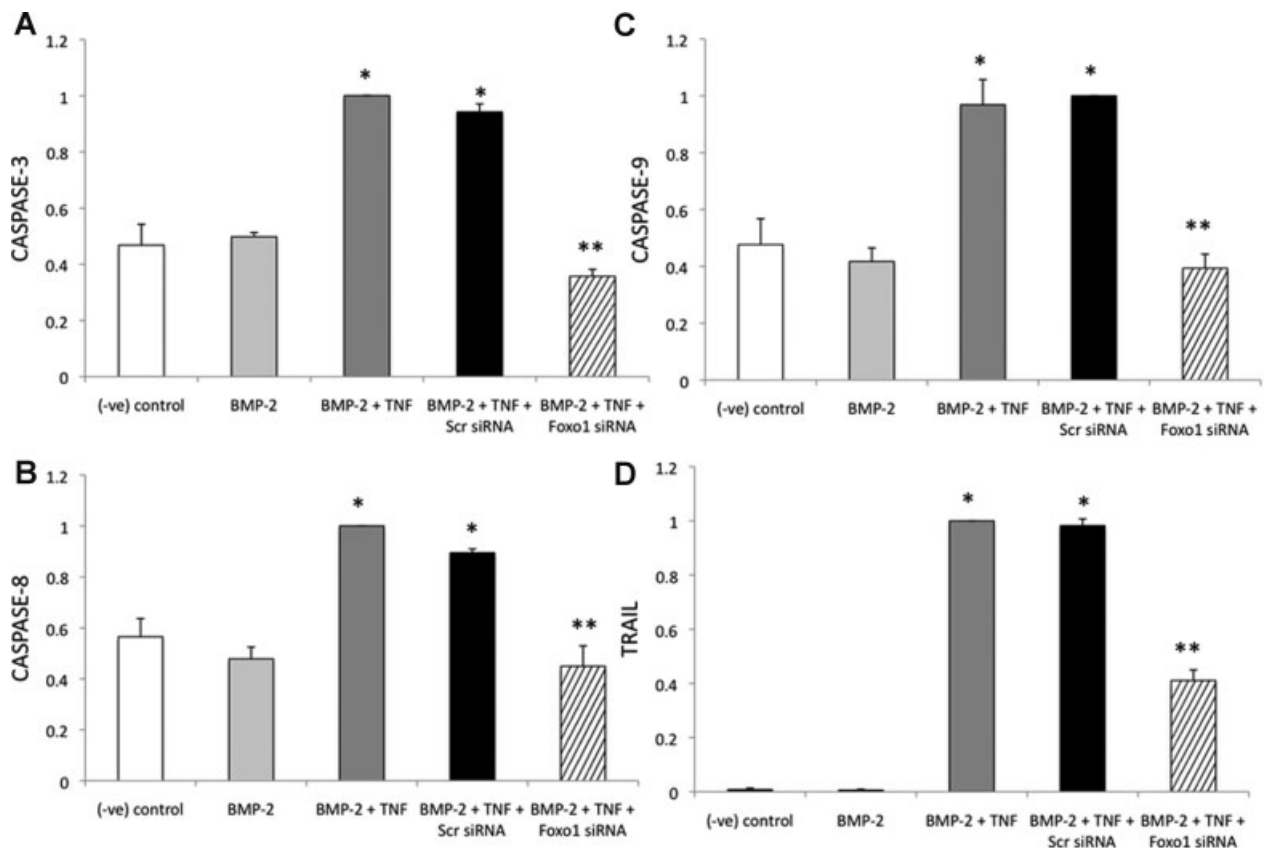


Fig. 4. *FOXO1* siRNA decreases TNF- α -induced apoptosis in BMP-2-stimulated cells at mRNA levels. ATDC5 cells were treated with BMP-2 and then stimulated with TNF- α . Cells treated with TNF- α were pretransfected with either *FOXO1*-specific or scrambled siRNA. Total mRNA levels of selected proapoptotic genes were tested by real-time PCR. (A) *Caspase-3*. (B) *Caspase-8*. (C) *Caspase-9*. (D) *TRAIL*. The data presented are the mean of three independent experiments \pm SEM and are shown as percent of maximum stimulation. *Significant increase with TNF- α stimulation ($p < .05$). **Significant reduction with *FOXO1* siRNA ($p < .05$).

To establish whether *caspase-8* and *caspase-9*, whose mRNA levels were regulated by *FOXO1*, played a prominent role in TNF- α -induced chondrocyte apoptosis, specific peptide inhibitors were used. Inhibition of *caspase-8* reduced TNF- α -stimulated apoptosis by approximately 40%, and inhibition of *caspase-9* reduced TNF- α -stimulated apoptosis by 50%, both of which were significant ($p < .05$). However, when both inhibitors were used together, apoptosis was reduced by 85% ($p < .05$), indicating that both caspases participate in the apoptotic process (Fig. 5). This suggests that the extracellular and intracellular apoptotic pathways are involved in mediating TNF- α -induced cell death in chondrogenic cells.

Selected results obtained with ATDC5 cells were confirmed with C3H10T1/2 cells. C3H10T1/2 cells were incubated with BMP-2 and differentiated to chondrogenic cells, as shown by several-fold induction of mRNA for *collagen II* and *collagen X* (data not shown). In the absence of BMP-2 stimulation, TNF- α did not stimulate apoptosis (Fig. 6A). However, when these cells acquired a chondrogenic phenotype, TNF- α stimulated a dose-dependent increase in apoptosis in both (Fig. 6B). When tested for induction of proapoptotic genes, TNF- α stimulated a 3- to 5-fold increase in *caspase-3*, *caspase-8*, and *caspase-9* mRNA levels and more than a 50-fold increase in *TRAIL* mRNA levels in C3H10T1/2 cells with a chondrogenic phenotype (Fig. 7). In each case, *FOXO1* siRNA

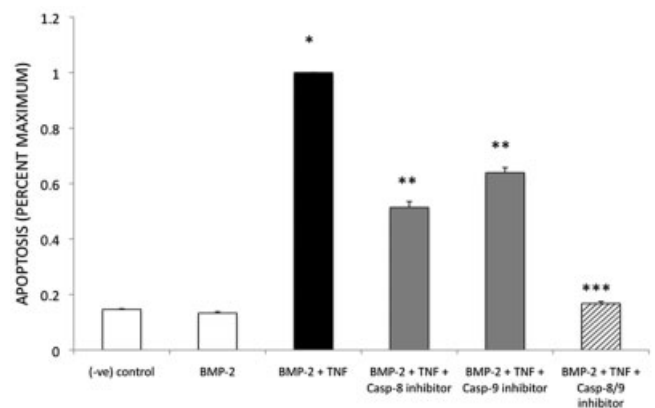


Fig. 5. Inhibition of apoptosis by inhibition of caspase-8 and caspase-9 in ATDC5 cells. ATDC5 cells were treated with BMP-2 and then stimulated with TNF- α . Cells then were treated with caspase-8 inhibitor or caspase-9 inhibitor or both. Apoptosis was measured by histone-associated cytoplasmic DNA. The data presented are the mean of three independent experiments \pm SEM and are shown as percent of maximum stimulation. *Significant increase with TNF- α stimulation ($p < .05$). **Significant reduction compared with TNF- α stimulation ($p < .05$). ***Significant reduction compared with treatment with one inhibitor ($p < .05$).

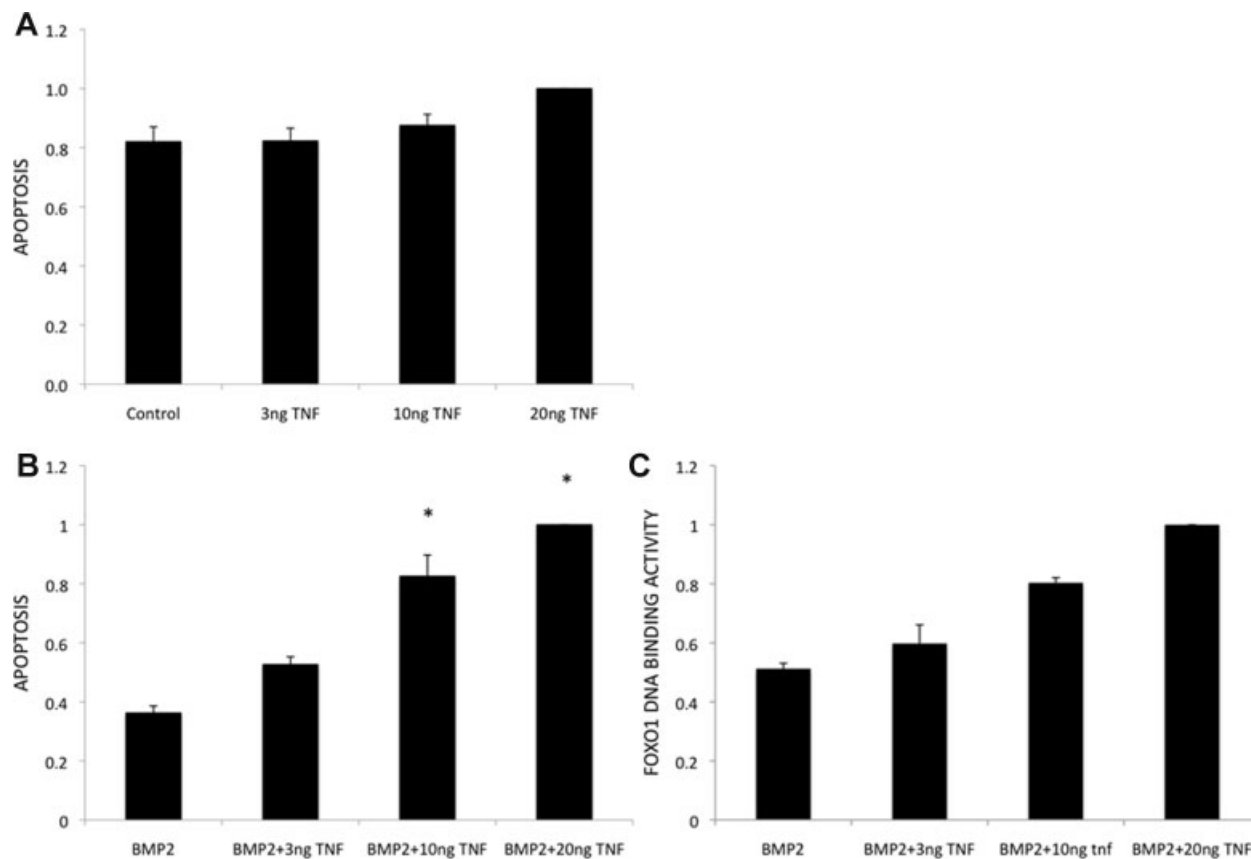


Fig. 6. TNF- α stimulates apoptosis in a dose-response manner in C3H10T1/2 cells only after they acquire a chondrogenic phenotype. Cells were grown with or without BMP-2 treatment and stimulated with TNF- α in a dose-response manner, and apoptosis and FOXO1 DNA binding were measured. (A) Apoptosis assay in undifferentiated C3H10T1/2 cells. (B) Apoptosis assay in differentiated C3H10T1/2 cells. (C) FOXO1 DNA-binding activity in differentiated C3H10T1/2 cells. The data presented are the mean of three independent experiments \pm SEM and are shown as percent of maximum stimulation. *Significant increase with TNF- α stimulation ($p < .05$).

knocked down the mRNA level by more than 60%, which was significant for each gene ($p < .05$). In control experiments, FOXO1 siRNA significantly knocked down TNF- α -stimulated FOXO1 mRNA levels by more than 80%, whereas scrambled siRNA had no effect (data not shown).

Discussion

Relatively little is known about the impact of diabetes on the transition from cartilage to bone during fracture healing. Our group has previously reported that diabetic fracture healing is associated with smaller calluses, premature loss of cartilage, and increased osteoclastic activity.^(13,27) Recently, we also have shown that inhibiting TNF- α reverses many of these effects.⁽²²⁾ We focused on a potentially important event, chondrocyte apoptosis. To investigate pathways that may affect apoptosis in diabetic animals, large-scale transcriptional profiling analysis was carried out on total RNA that was isolated from normal and diabetic callus tissue at various time points, and the nature of expressed genes was assessed by comparisons of gene expression sets that were preferentially observed in the two sets of callus tissues. These results showed that diabetes caused the upregulation of several apoptotic pathways, particularly

during the transition from cartilage to bone on day 16. The upregulation of apoptotic pathways agreed well with the increase in caspase-3 activity noted in the diabetic group and the enhanced number of apoptotic chondrocytes. At an earlier time point, there was no upregulation of apoptotic gene sets or chondrocyte apoptosis in the diabetic group. This may be significant because enhanced or premature chondrocyte cell death may trigger subsequent events that accelerate degradation of cartilage.⁽¹⁷⁾ It was shown in articular chondrocytes that TNF- α -induced apoptosis was associated with increased expression of genes related to matrix degradation such as MMP and macrophage colony stimulating factor (MCSF).⁽³⁸⁾ Similarly, in the absence of TNF- α during bone repair, expression of these genes is downregulated.⁽³⁹⁾ This link is supported by findings that mRNA levels of MCSF and other proresorptive cytokines are also elevated on day 16 in diabetic compared with normal animals.⁽¹³⁾

High levels of TNF have been linked to a number of osseous disorders, including osteoporosis, osteolysis, osteoarthritis, and rheumatoid arthritis.⁽⁴⁰⁻⁴²⁾ At both the mRNA and protein levels, diabetes caused a significant increase in TNF- α during fracture healing. Chondrocytes are particularly sensitive to TNF-induced apoptosis,^(38,43) consistent with results that TNF alone stimulated apoptosis in C3H10T1/2 cells with a BMP-2-induced chondrogenic phenotype but not in undifferentiated C3H10T1/2

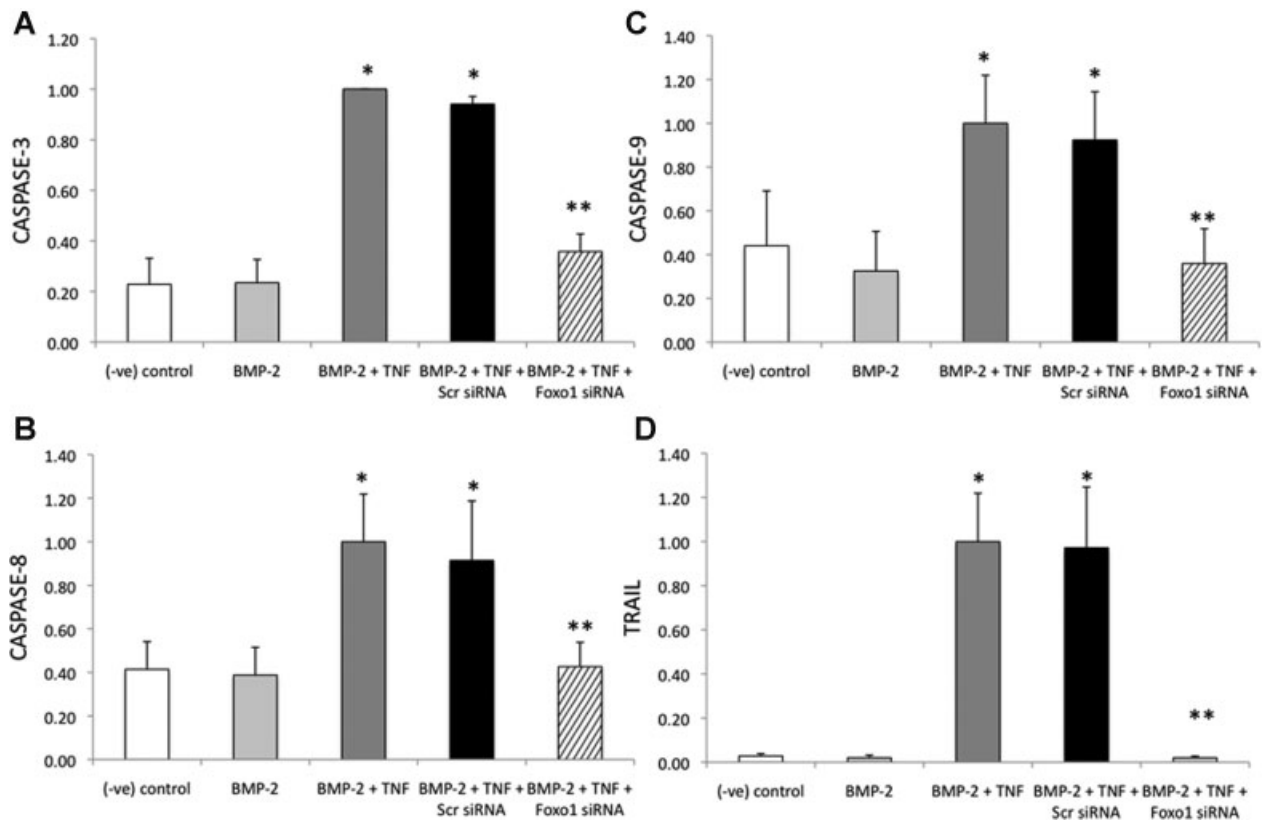


Fig. 7. *FOXO1* siRNA decreases TNF- α -induced apoptosis in BMP-2-stimulated cells at mRNA levels. C3H10T1/2 cells were treated with BMP-2 and then stimulated with TNF- α . Cells treated with TNF- α were pretransfected with either *FOXO1*-specific or scrambled siRNA. Total mRNA levels of selected proapoptotic genes were tested by real-time PCR. (A) *Caspase-3*. (B) *Caspase-8*. (C) *Caspase-9*. (D) *TRAIL*. The data presented are the mean of three independent experiments \pm SEM and are shown as percent of maximum stimulation. *Significant increase with TNF- α stimulation ($p < .05$). **Significant reduction with *FOXO1* siRNA ($p < .05$).

mesenchymal cells. When diabetic mice were treated with a TNF-specific inhibitor, we noted a significant reduction in chondrocyte apoptosis in diabetic mice but not in normoglycemic mice. This would indicate that the increase in TNF- α is particularly important in the diabetic animals and drives apoptosis of chondrocytes. In parallel studies, TNF- α was produced at the highest levels in hypertrophic chondrocytes in diabetic calluses during fracture repair (data not shown). This would suggest an autocrine mechanism for TNF-stimulated apoptosis of hypertrophic chondrocytes. We have previously reported that when TNF receptor signaling is completely abrogated by genetic deletion, chondrocyte apoptosis is delayed, and we have postulated that this delay interferes with fracture healing.⁽⁴⁴⁾ In vivo and in vitro experiments performed here indicate that TNF plays a role in the expression of proapoptotic genes enhanced by diabetes and that TNF-stimulated apoptosis in chondrocytes is mediated by FOXO1. It is possible that this occurs through an autocrine mechanism because we previously reported that chondrocytes in diabetic fracture healing exhibit increased expression of TNF- α in vivo,⁽²²⁾ and others have shown that chondrocytes undergoing apoptosis in vivo express caspase 3 and 9, both of which are targets of FOXO1.^(19,45,46) These results indicate the TNF initiates the early phase of chondrocyte apoptosis, but at the later phases, other factors such as FasL are more likely to have a significant role in chondrocyte apoptosis in normoglycemic animals.

It has been shown in vivo that diabetes increases FOXO1 DNA-binding activity and increases FOXO1 nuclear translocation in chondrocytes in fracture repair.⁽²²⁾ This is also shown in this study, but when TNF was inhibited, FOXO1 nuclear translocation was reduced, which may indicate that the effects of TNF on apoptosis is mediated through FOXO1. To investigate further the mechanism by which TNF could induce chondrocyte apoptosis, in vitro studies were carried out. Two cell lines with a BMP-2-induced chondrogenic phenotype were examined and produced similar results. TNF- α stimulated apoptosis and proapoptotic gene expression in both chondrogenic cells that was significantly reduced by FOXO1 knockdown. Interestingly, TNF did not induce apoptosis in undifferentiated C3H10T1/2 cells (Fig. 6) and did not enhance mRNA levels in the undifferentiated cells (unpublished data). Thus the acquisition of a chondrogenic phenotype renders cells sensitive to TNF- α -induced apoptosis and FOXO1 activation, consistent with knockdown experiments in which FOXO1 played an important role in mediating TNF-induced apoptosis and proapoptotic gene expression. FOXO1 induces the expression of a large number of proapoptotic extracellular and intracellular mediators such as FasL, TRAIL, and caspases.^(19,47) Because of the increased expression of proapoptotic factors, caspase activity is also increased, and apoptosis is induced.^(19,47) In the present study, silencing FOXO1 in chondrogenic cells not only inhibited apoptosis but also inhibited *TRAIL*, *caspase-3*, *caspase-8*, and *caspase-9*.

Diabetes-enhanced apoptosis is associated with diabetic complications. Diabetes increases the rate of fibroblast apoptosis stimulated by a bacteria-induced wound, and the higher level of apoptosis contributes to an impaired wound-healing response.⁽⁴⁸⁾ There is also evidence of increased apoptosis of pericytes and endothelial cells in retinas of diabetic animals, which was found to be a contributing factor to diabetic retinopathy and caused in part by increased levels of TNF.^(49–52) Thus TNF dysregulation caused by diabetes may affect a number of different tissues, including cartilage, during fracture healing. This may lead to greater chondrocyte apoptosis, which potentially could affect the cartilage in the diabetic animals. It is striking that diabetic fracture healing is also characterized by increased production of proresorptive factors and accelerated formation of osteoclasts and cartilage degradation.^(13,27)

Disclosures

All the authors state that they have no conflicts of interest.

Acknowledgments

This work was supported by NIH Grants P01AR49920 (TAE) and R01DE017732 (DTG) and Grant DAMD17-03-0576 (LCG).

References

- Jehle PM, Jehle DR, Mohan S, Bohm BO. Serum levels of insulin-like growth factor system components and relationship to bone metabolism in type 1 and type 2 diabetes mellitus patients. *J Endocrinol*. 1998;159:297–306.
- Kemink SA, Hermus AR, Swinkels LM, Lutterman JA, Smals AG. Osteopenia in insulin-dependent diabetes mellitus; prevalence and aspects of pathophysiology. *J Endocrinol Invest*. 2000;23:295–303.
- Piepkorn B, Kann P, Forst T, Andreas J, Pfutzner A, Beyer J. Bone mineral density and bone metabolism in diabetes mellitus. *Horm Metab Res*. 1997;29:584–591.
- Tuominen JT, Impivaara O, Puukka P, Ronnema T. Bone mineral density in patients with type 1 and type 2 diabetes. *Diabetes Care*. 1999;22:1196–1200.
- Hamada Y, Kitazawa S, Kitazawa R, Fujii H, Kasuga M, Fukagawa M. Histomorphometric analysis of diabetic osteopenia in streptozotocin-induced diabetic mice: a possible role of oxidative stress. *Bone*. 2007;40:1408–1414.
- Thraill KM, Liu L, Wahl EC, et al. Bone formation is impaired in a model of type 1 diabetes. *Diabetes*. 2005;54:2875–2881.
- Hie M, Shimono M, Fujii K, Tsukamoto I. Increased cathepsin K and tartrate-resistant acid phosphatase expression in bone of streptozotocin-induced diabetic rats. *Bone*. 2007;41:1045–1050.
- Kawashima Y, Fritton JC, Yakar S, et al. Type 2 diabetic mice demonstrate slender long bones with increased fragility secondary to increased osteoclastogenesis. *Bone*. 2008.
- Cozen L. Does diabetes delay fracture healing? Does diabetes delay fracture healing? *Clin Orthop*. 1972;82:134–140.
- Loder R. The influence of diabetes mellitus on the healing of closed fractures. *Clin Orthop*. 1988; (232) Review: 210–216.
- Dixit P, Ekstrom R. Retardation of bone fracture healing in experimental diabetes. *Indian J Med Res*. 1987;85:426–435.
- Beam H, Parsons J, Lin S. The effects of blood glucose control upon fracture healing in the BB Wistar rat with diabetes mellitus. *J Orthop Res*. 2002;20:1210–1216.
- Kayal RA, Tsatsas D, Bauer MA, et al. Diminished bone formation during diabetic fracture healing is related to the premature resorption of cartilage associated with increased osteoclast activity. *J Bone Miner Res*. 2007;22:560–568.
- Ogasawara A, Nakajima A, Nakajima F, Goto K, Yamazaki M. Molecular basis for affected cartilage formation and bone union in fracture healing of the streptozotocin-induced diabetic rat. *Bone*. 2008;43:832–839.
- Lee FY, Choi YW, Behrens FF, DeFouw DO, Einhorn TA. Programmed removal of chondrocytes during endochondral fracture healing. *J Orthop Res*. 1998;16:144–150.
- Komatsu DE, Bosch-Marce M, Semenza GL, Hadjiargyrou M. Enhanced bone regeneration associated with decreased apoptosis in mice with partial HIF-1alpha deficiency. *J Bone Miner Res*. 2007; 22:366–374.
- Gibson G. Active role of chondrocyte apoptosis in endochondral ossification. *Microsc Res Tech*. 1998;43:191–204.
- Gibson G, Kohler W, Schaffler M. Chondrocyte apoptosis in endochondral ossification of chick sterna. *Dev Dyn*. 1995;203:468–476.
- Alikhani M, Alikhani Z, Graves DT. FOXO1 functions as a master switch that regulates gene expression necessary for tumor necrosis factor-induced fibroblast apoptosis. *J Biol Chem*. 2005;280:12096–12102.
- Furukawa-Hibi Y, Kobayashi Y, Chen C, Motoyama N. FOXO transcription factors in cell-cycle regulation and the response to oxidative stress. *Antioxid Redox Signal*. 2005;7:752–760.
- Alikhani M, MacLellan CM, Raptis M, Vora S, Trackman PC, Graves DT. Advanced glycation end products induce apoptosis in fibroblasts through activation of ROS, MAP kinases, and the FOXO1 transcription factor. *Am J Physiol Cell Physiol*. 2007;292:C850–856.
- Alblowi J, Kayal RA, Siqueira M, et al. High Levels of TNF- α Contribute to Accelerated Loss of Cartilage in Diabetic Fracture Healing. *Am J Pathol*. in press.
- Burgering D, Medema R. Decision on life and death: FOXO Forkhead transcription factors are in command when PKB/Akt is off duty. *J Leuko Biol*. 2003;73:689–701.
- Gilley J, Coffey PJ, Ham J. FOXO transcription factors directly activate bim gene expression and promote apoptosis in sympathetic neurons. *J Cell Biol*. 2003;162:613–622.
- Brunet A, Bonni A, Zigmond MJ, et al. Akt promotes cell survival by phosphorylating and inhibiting a Forkhead transcription factor. *Cell*. 1999;96:857–868.
- Behl Y, Siqueira M, Ortiz J, et al. Activation of the acquired immune response reduces coupled bone formation in response to a periodontal pathogen. *J Immunol*. 2008;181:8711–8718.
- Kayal RA, Alblowi J, McKenzie E, et al. Diabetes causes the accelerated loss of cartilage during fracture repair which is reversed by insulin treatment. *Bone*. 2009;44:357–363.
- Gerstenfeld LC, Alkhiary YM, Krall EA, et al. Three-dimensional reconstruction of fracture callus morphogenesis. *J Histochem Cytochem*. 2006;54:1215–1228.
- Gerstenfeld LC, Wronski TJ, Hollinger JO, Einhorn TA. Application of histomorphometric methods to the study of bone repair. *J Bone Miner Res*. 2005;20:1715–1722.
- Wang K, Vishwanath P, Eichler GS, et al. Analysis of fracture healing by large-scale transcriptional profile identified temporal relationships between metalloproteinase and ADAMTS mRNA expression. *Matrix Biol*. 2006;25:271–281.
- Subramanian A, Tamayo P, Mootha VK, et al. Gene set enrichment analysis: a knowledge-based approach for interpreting genome-wide expression profiles. *Proc Natl Acad Sci U S A*. 2005;102:15545–15550.

32. Dasu MR, Barrow RE, Herndon DN. Gene expression changes with time in skeletal muscle of severely burned children. *Ann Surg.* 2005;241:647–653.
33. Reddi AH. Role of morphogenetic proteins in skeletal tissue engineering and regeneration. *Nat Biotechnol.* 1998;16:247–252.
34. Ju W, Hoffmann A, Verschuere K, et al. The bone morphogenetic protein 2 signaling mediator Smad1 participates predominantly in osteogenic and not in chondrogenic differentiation in mesenchymal progenitors C3H10T1/2. *J Bone Miner Res.* 2000;15:1889–1899.
35. Atsumi T, Miwa Y, Kimata K, Ikawa Y. A chondrogenic cell line derived from a differentiating culture of AT805 teratocarcinoma cells. *Cell Differ Dev.* 1990;30:109–116.
36. Shukunami C, Ohta Y, Sakuda M, Hiraki Y. Sequential progression of the differentiation program by bone morphogenetic protein-2 in chondrogenic cell line ATDC5. *Exp Cell Res.* 1998;241:1–11.
37. Hirao M, Tamai N, Tsumaki N, Yoshikawa H, Myoui A. Oxygen tension regulates chondrocyte differentiation and function during endochondral ossification. *J Biol Chem.* 2006;281:31079–31092.
38. Cho TJ, Lehmann W, Edgar C, et al. Tumor necrosis factor alpha activation of the apoptotic cascade in murine articular chondrocytes is associated with the induction of metalloproteinases and specific pro-resorptive factors. *Arthritis Rheum.* 2003;48:2845–2854.
39. Lehmann W, Edgar CM, Wang K, et al. Tumor necrosis factor α (TNF- α) coordinately regulates the expression of specific matrix metalloproteinases (MMPs) and angiogenic factors during fracture healing. *Bone.* 2005;36:300–310.
40. Saldenber-Kermanac'h N, Corrado A, Lemeiter D, deVernejoul MC, Boissier MC, Cohen-Solal ME. TNF- α antibodies and osteoprotegerin decrease systemic bone loss associated with inflammation through distinct mechanisms in collagen-induced arthritis. *Bone.* 2004; 35: 1200–1207.
41. Liu R, Bal HS, Desta T, Behl Y, Graves DT. Tumor necrosis factor- α mediates diabetes-enhanced apoptosis of matrix-producing cells and impairs diabetic healing. *Am J Pathol.* 2006;168:757–764.
42. Taylor PC. Anti-TNF therapy for rheumatoid arthritis and other inflammatory diseases. *Mol Biotechnol.* 2001;19:153–168.
43. Aizawa T, Kon T, Einhorn TA, Gerstenfeld LC. Induction of apoptosis in chondrocytes by tumor necrosis factor- α . *J Orthop Res.* 2001;19:785–796.
44. Gerstenfeld LC, Cho TJ, Kon T, et al. Impaired fracture healing in the absence of TNF- α signaling: the role of TNF- α in endochondral cartilage resorption. *J Bone Miner Res.* 2003;18:1584–1592.
45. Matsuo M, Nishida K, Yoshida A, Murakami T, Inoue H. Expression of caspase-3 and -9 relevant to cartilage destruction and chondrocyte apoptosis in human osteoarthritic cartilage. *Acta Med Okayama.* 2001;55:333–340.
46. Dang AC, Kim HT. Chondrocyte apoptosis after simulated intra-articular fracture: a comparison of histologic detection methods. *Clinical Orthopaedics and Related Research.* 2009;467:1877–1884.
47. Huang H, Tindall DJ. Dynamic FoxO transcription factors. *J Cell Sci.* 2007;120:2479–2487.
48. Al-Mashat HA, Kandru S, Liu R, Behl Y, Desta T, Graves DT. Diabetes enhances mRNA levels of proapoptotic genes and caspase activity, which contribute to impaired healing. *Diabetes.* 2006;55:487–495.
49. Mohr S, Xi X, Tang J, Kern TS. Caspase activation in retinas of diabetic and galactosemic mice and diabetic patients. *Diabetes.* 2002; 51: 1172–1179.
50. Romeo G, Liu W-H, Asnaghi V, Kern TS, Lorenzi M. Activation of Nuclear Factor- κ B Induced by Diabetes and High Glucose Regulates a Proapoptotic Program in Retinal Pericytes. *Diabetes.* 2002;51:2241–2248.
51. Barber AJ. A new view of diabetic retinopathy: a neurodegenerative disease of the eye. *Prog Neuropsychopharmacol Biol Psychiatry.* 2003;27:283–290.
52. Barber AJ, Antonetti DA, Kern TS, et al. The Ins2Akita mouse as a model of early retinal complications in diabetes. *Invest Ophthalmol Vis Sci.* 2005;46:2210–2218.